Journal of Machine Engineering, 2026, Vol. 26
ISSN 1895-7595 (Print) ISSN 2391-8071 (Online)

Received*: 09 February 2026* / Accepted: *27 April 2026* / Published online: *18 May 2026*

machining, simulation,
residual stress,
cold forming

Radu Andrei MATEI[1*], Cornelius NEUN[2],
Mathias LIEWALD[3], Hans-Christian MÖHRING[4],
Marco SPETH[1]

NUMERICAL AND EXPERIMENTAL INVESTIGATION OF RESIDUAL-STRESS-INDUCED DISTORTIONS IN COLD FORGED EN AW-6082 ALUMINIUM SPECIMENS AFTER TARGETED MILLING

Near-net-shape (NNS) cold forging offers significant potential for material savings compared to processes like machining from solid billets. However, this process introduces residual stress (RS) fields that can cause distortions during subsequent machining. Predicting and controlling these distortions is essential for ensuring dimensional accuracy and minimizing scrap rates in industrial applications. This study investigates the distortions caused by targeted milling operations on extruded aluminium cross-shaped specimens made from an EN AW-6082 aluminium alloy. The aim is the determination of the predictive capabilities of machining-induced distortions from RS liberation by commercial FEM software. Elastoplastic FEM simulations of the complete operation chain are developed using DEFORM 3D. Boolean operations combined with RS relaxation are used to simulate the milling operations in a simplified way. The numerical results are validated experimentally using systematic milling tests and software-aligned 3D scans of the specimens at all tested milling depths. The results are in good agreement, with simulations showing an average discrepancy of 22% with respect to experiments, good distortion mode prediction and the capture of observed trends in the influence of milling depth. However, a more accurate and repeatable alignment strategy is required for a higher confidence in the predictions.

1. INTRODUCTION

The Priority Program 2476 of the German Research Foundation (DFG SPP2476) aims to reformulate process chain design as an inverse problem under stochastic uncertainties. Inverse cross-process optimization enables a transition from local improvements to a holistic view, balancing technical, ecological and economic goals while ensuring final component specifications are met. The investigation reported about in this paper is a collaborative work

[1] Department of Bulk Metal Forming, Institute for Metal Forming Technology, University of Stuttgart, Germany
[2] Cutting Department, Institute for Machine Tools, University of Stuttgart, Germany
[3] Management, Institute for Metal Forming Technology, University of Stuttgart, Germany
[4] Management, Institute for Machine Tools, University of Stuttgart, Germany
[*] E-mail: radu-andrei.matei@ifu.uni-stuttgart.de
https://doi.org/10.36897/jme/221154

between the Institute for Metal Forming Technology (IFU) and the Institute for Machine Tools (IfW) of the University of Stuttgart.

In ProMoKaZ (German acronym for "Cross-process modelling of a cold forging and machining process chain of an impeller wheel with consideration of specific uncertainties") a two-stage process chain consisting of forming a Near-Net-Shape (NNS) centrifugal impeller from EN AW-6082 aluminium and machining it to final specifications is investigated. HeliForm [1] is a novel forming process developed at the IFU in which an NNS centrifugal impeller preform is manufactured in a single forming stroke, as presented in Fig. 1. The blades and central hub are formed using a forward extrusion process while the complex curvature of the blades is given during the ejection by precisely turning the extrusion die with a motor and transmission system. This allows for potential reductions in initial material volume of more than 50%, with the associated reductions in CO2 emissions and cost the initial material accounts for. The main objectives for the first funding period of ProMoKaZ are to develop the physical process chain, to model the process chain in an inverse way with fast surrogate models and to quantify the process chain uncertainties and their propagation.

HeliForm introduces inhomogeneous plastic strain and cooling inside of the component, which generates a complex state of forming residual stresses (RS) in the part. As the preform blades must be machined to final thickness on both sides, a critical interaction between the stages are the RS, which make the blades deflect as they are being milled. In the present investigation, the capabilities of the commercial FEM program DEFORM 3D in its 14.1 version for predicting the distortions generated when targeted milling operations liberate forming RS are assessed.

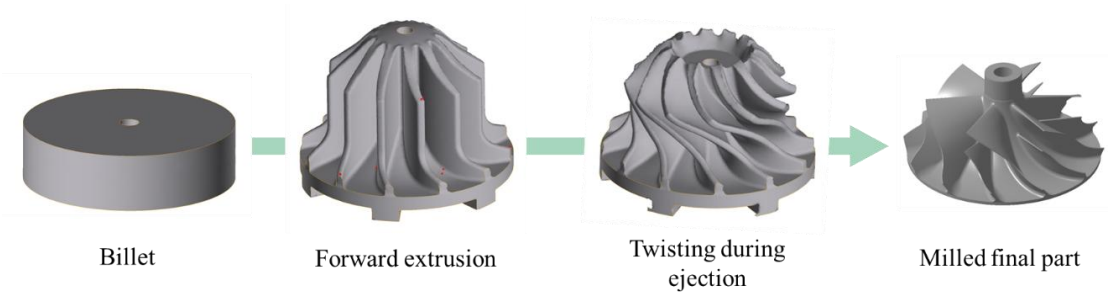

Fig. 1. New HeliForm process for the production of centrifugal impellers

2. STATE OF THE ART

RS are the internal, non-zero stress state of a component when no significant external loads are applied on it. Metallic components such as aluminium and steel usually present such RS fields as a consequence of their manufacturing processes. Forming, casting or heat treatments generate RS fields across the whole part thickness, which are known as bulk residual stresses (BRS) [2]. The equilibrium of these RS is disturbed when material is removed to achieve the final geometry to be produced, which distorts the part as it finds a new equilibrium of internal stresses. In addition, the material removal process usually introduces new RS into the part. These only affect a small superficial region and are known

as Machining-Induced RS (MIRS). MIRS become especially relevant in metallic thin-walled components (with wall thicknesses lower than 4-5 mm), especially made from aluminium alloys such as the investigated NNS impeller and the simplified cross specimen [2].

Measurement of RS fields is to this day time-consuming, costly and research-oriented. According to [2], the main method used in the literature for experimental determination of BRS is the layer removal method. It consists of the chemical removal of thin layers of material such that the modification of the existing RS field is minimal or even negligible. Other methods include the contour method, neutron diffraction, deep hole drilling or the ultrasonic method. In the case of MIRS, the main methods cited in the literature are X-ray diffraction (XRD), neutron diffraction and hole-drilling. These methods vary mainly in their cost, damage to the part, measurement accuracy and depth of measurement [2, 3].

Prediction of RS fields is done mainly by FEM simulations [3], although this is a time-consuming process, especially regarding the prediction of MIRS [2]. Some commonly used tools for predicting the effects of RS when the thermomechanical effects of machining are not of interest or are negligible are boolean operations [24–26]. In boolean operations the material to be machined is removed at once, the geometry remeshed, and the part is allowed to relax and distort; or the element death and birth method, in which a more realistic simulation of machining passes is performed [2]. FEM is also integral to the contour method, a destructive technique for experimental RS measurement. It consists of making precise cuts (typically by wire EDM) on the specimens of interest to reveal highly planar internal cross-sections. As the BRS are liberated, the initially planar cross-sections distort. These deviations are measured by CMM and then entered into FEM simulations as displacement boundary conditions on the revealed cross sections and the stresses they produce are considered the measured BRS [2].

RS in cold forging originate from inhomogeneous plastic deformation and thermal gradients. Modern paradigms shift from merely shaping components to actively designing RS distributions [4]. This is achieved by manipulating specific process kinematics, tool geometries, hydrostatic and deviatoric stress states or lubrication conditions, which can have significant effects on the homogenization of strain fields or the alteration of surface shear stresses. Furthermore, the ejection stage can be strategically utilized to redistribute the stress profile. While cold forging can have positive impacts like the improvement of fatigue life thanks to compressive surface RS, unmanaged bulk RS remain one of the primary causes of macroscopic geometric distortion during subsequent machining or heat treatment [5].

Many further studies comprehensively investigate RS simulation, especially in the field of machining, specifically in milling and turning. In machining, many parameters have an influence on the process and quality variables as well as on the RS state of the workpiece. The numerical simulation of chip formation processes for the prediction of process forces and temperatures, RS and boundary zone properties as well as component distortion is the subject of numerous current research projects. The use of the classical Lagrangian approach, the coupled Euler-Lagrange approach (CEL) in the FEM and mesh-free methods are described in [6]. In [7], a process-induced RS depth profile is compared with the forces of an orthogonal cut for AISI 4140. [8] presents an approach for predicting deflections of thin-walled components during a milling process. A Fourier series approach is used to make the calculation real-time capable. In [9], the machining forces and stresses are used to calculate the form deviation. In [10] an investigation of component deformations caused by residual

forging stresses, which are relieved by subsequent machining, is presented. Hasan et al. present an uncertainty quantification based on the Monte Carlo method and investigate how material parameters and friction affect the RS in the machining of Inconel 718 [11]. In [12] soft sensors are used in closed loop control to predict the microstructure and RS from sensor data and to improve process control. In the project SPP 2086, a sensory drilling tool was developed that enables the thermomechanical process load collective to be recorded close to the point of action. An FE-based soft sensor can be used to infer the temperature at the workpiece-tool contact point [13, 14]. Correlations between process variables and measured and simulated RS states enable edge zone-related process control. In further work, correlations between the properties of milled surfaces and acceleration data of a sensor-based milling tool were investigated [15]. In [16], the influence of varying Johnson Cook (JC) parameters on the simulated cutting force is shown. AI regression models are trained to predict process properties independently of the machining simulation. Uncertainties due to scattering material conditions can be eliminated by inverse adjustment of the JC parameters. The influence of varying cutting edge geometries was investigated in FE analyses of temperature and residual stress formation.

No other studies have been found that systematically analyse the capabilities of a commercial FEM software like DEFORM 3D for predicting the 3D distortions in complex, thin-walled, extruded aluminium components induced by cyclically symmetric milling while validating these results experimentally with 3D optical scanning. This is the research gap addressed in the present investigation.

3. DESCRIPTION OF INVESTIGATIONS

3.1. EXPERIMENTAL SETUP

3.1.1. DESCRIPTION OF THE COMPONENT, FORMING TOOL AND MATERIAL CHARACTERIZATION

The component used in the present study is a forward-extruded workpiece with a cross-shaped cross section. The extrusion was performed at room temperature. The geometry, presented in Fig. 2a, was designed as a simplified version of the NNS impeller wheel for the preliminary torsional tests performed in the HeliForm project (see Fig. 1). The main dimensions of the specimen are presented in Fig. 2b. The billet material is EN AW-6082 aluminium and it was fully annealed prior to the extrusion. The blanks were prepared for lubrication using sandblasting and were lubricated with zinc stearate in a tumbler, ensuring a thin homogeneous coating of approximately 5g/m2. The tool used for the extrusion of the component is presented in Fig. 2c. It was mounted on a Muller 200-ton hydraulic press. The stroke was kept constant at 13.2 mm using distance columns with metal sheets of precise thickness for fine stroke adjustment. The elastoplastic behaviour of the material was characterized using compression tests. Cylindrical specimens of 10 mm in diameter and 15 mm in height were compressed to a true strain of 0.8 using a Gleeble 3800c thermomechanical simulator while capturing the force-displacement data with an integrated data acquisition

system. True stress-strain curves were computed from the raw data using a Python code with automatic temperature compensation. The final flow curves were integrated into the material card of the DEFORM 3D simulations of the extrusion process.

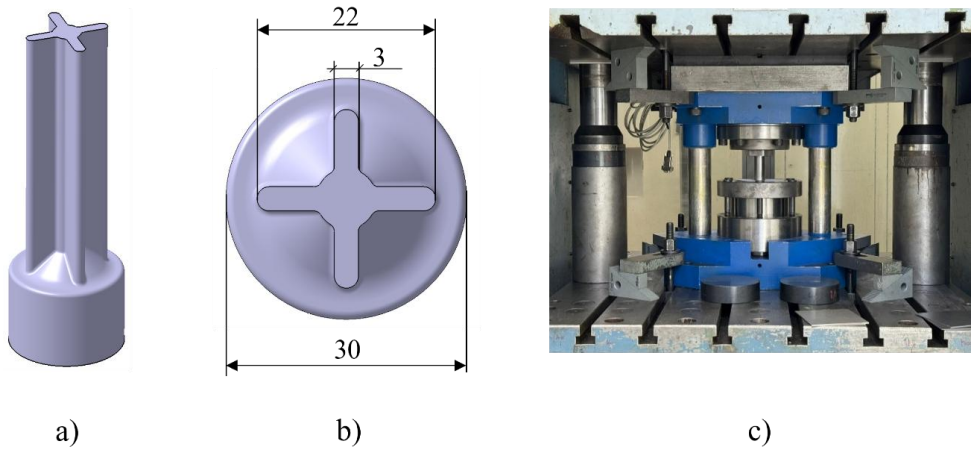

Fig. 2. Specimen geometry (a), dimensions (in mm) of the extruded cross-section (b) and used forming tool (c)

3.1.2. DESCRIPTION OF THE SYSTEMATIC MILLING OF THE PARTS

The objective of the milling operation in this study is to progressively remove material from the forged billets so that the release of forming-induced bulk residual stresses produces measurable distortion. The distortion signal we seek to quantify arises from two contributions which must be clearly distinguished: (i) the pre-existing bulk residual stress field, introduced during the forging process and retained throughout the entire cross-section of the billet, which is the quantity of interest; and (ii) the machining-induced residual stress (MIRS) field, which is confined to a shallow layer (typically 50–200 µm in depth for aluminium alloys [18,19]) beneath the newly generated surface. To obtain an unambiguous distortion signal attributable to (i), the contribution from (ii) must be kept small and — importantly — of known sign and origin.

It is well established that the MIRS of milled aluminium alloys follows a hook-shaped profile, often referred to in the literature as a √-shaped profile [17,18,19], with a compressive maximum located at a depth of approximately 30–60 µm and a penetration depth on the order of 50–200 µm depending on feed per tooth and tool geometry [18, 19]. The sign and magnitude of the near-surface MIRS depend strongly on the balance between the mechanical and thermal loads imposed by the cutting process: at low cutting speeds the mechanical component dominates, producing shallow compressive MIRS [20]; at conventional milling speeds for aluminium (500–900 m/min) the thermal component becomes dominant, producing tensile MIRS that can reach magnitudes comparable to the distortion signal of interest [21, 22]. Recent experimental work on EN AW-2024 T351 demonstrates this transition: at v_c = 150 m/min the surface MIRS is close to zero or slightly compressive [22], whereas at v_c = 750 m/min it reaches approximately +350 MPa (tensile) [21]. The same transition has been shown theoretically by Wan et al. [23] in Ti-6Al-4V, where thermal loading was found to have weak influence on MIRS at low cutting velocities and a significant

influence only at high spindle speeds. It is precisely this transition that explains why the HSC regime, although productivity-optimal, is MIRS-maximizing rather than MIRS-minimizing.

For this reason, the cutting parameters in this study were deliberately selected to remain in the mechanically-dominated regime. Milling was carried out on a DECKEL FP4 with a GARANT HPC solid carbide end mill (d = 8 mm, three flutes, ZOX coating), at a spindle speed of n = 400 min^{-1}, corresponding to a cutting speed of $v\_c \approx 10$ m/min, with a feed rate v_f = 400 mm/min (f_z = 0.33 mm/tooth), a width of cut a_e = 7 mm (a_e/d = 0.875), and a depth of cut a_p = 0.5 mm per pass. Climb-cut (down-milling) was used throughout. A water-miscible emulsion-based cutting fluid was supplied manually as a continuous stream at approximately 1 l/min. The strategy of material removal is illustrated in Fig. 3. Because each pass removes 0.5 to 1.5 mm of material across the full cross-section, the volume of material relieved per increment — and hence the bulk strain energy released – exceeds the volume of the MIRS-affected surface layer by more than an order of magnitude. Consequently, the distortion signal of interest is dominated by the release of the bulk residual stress field, not by the MIRS layer introduced by the cutter, and strict control of the bulk thermal load during milling is therefore not required for the validity of the measurement.

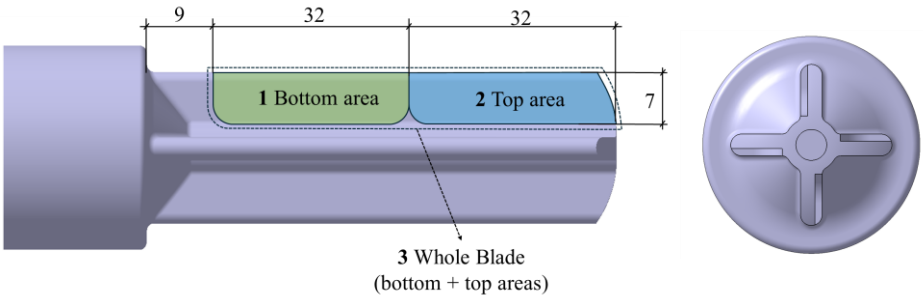

Fig. 3. Dimensions (in mm) and geometry of the three areas of milling operation performed on the specimens

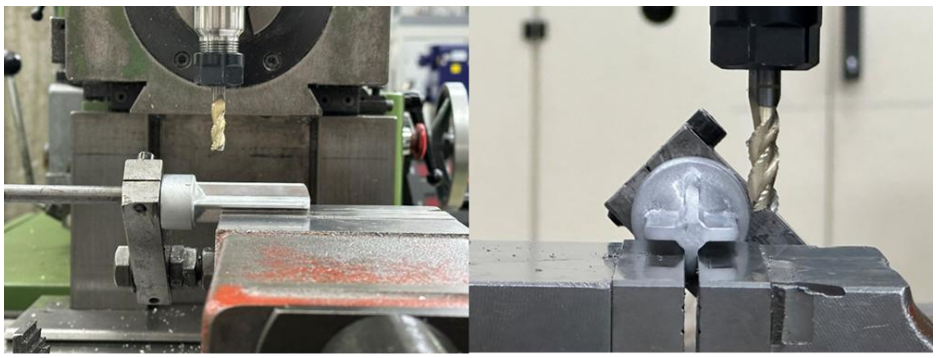

a) b)

Fig. 4. Milling setup with workpiece clamping. Side view (a) and front view (b).

3.1.3. PART SCANNING AND SCAN ALIGNMENT

The as-formed specimens were 3D scanned using a Keyence VR6000 optical 3D profilometer. The profilometer's rotation module was used to rotate the part 360º around its longitudinal axis (see Fig. 5). This method presented some limitations, mainly the inability to

capture surfaces and features perpendicular to the longitudinal axis of the part. Another limitation of the method is the misalignment of the scans. The 3D scans were exported as .stl meshes and post-processed using Zeiss Inspect 2026. All meshes were smoothed for improve alignment and visualization using a surface tolerance value of 0.005 mm (around an order of magnitude below the average distortions). The scans of the processed parts were aligned to a CAD model (due to poor alignment quality with as-formed meshes) of the specimen using a local best fit based on alignment references. The unextruded billet, extrusion shoulder and central cylinder were selected as references due to their high rigidity and expected negligible deflection. The alignment quality was determined using surface comparisons and deemed acceptable when the references showed close-to-zero surface deviations. This alignment strategy gave the most reliable results but cannot guarantee a negligible influence of the alignment on the observed distortions.

a) b)

Fig. 5. Keyence VR6000 (a) and 360º scanning setup using the rotational module (b)

3.2. FE SIMULATIONS

3.2.1. DESCRIPTION OF FE MODEL FOR EXTRUSION SIMULATION

The extrusion process was modelled using the FE software DEFORM 3D. A chained multioperation model was created for describing the forward extrusion, ejection, cooling and relaxation of the specimen. The geometries for all forming operations are shown in Fig. 6. The billet was modelled as a 45º slice of the actual geometry for taking advantage of the final part symmetries. Symmetry boundary conditions were added to the nodes on the symmetry planes. The workpiece was set as an elastoplastic body using the material card developed from the material characterization. The die was defined as a rigid object with realistic extrusion die relief and heat transfer. Die temperature increases were neglected for faster computation. A tetrahedral mesh with an initial number of elements of 113971 was used to discretize the blank. The element number was allowed to grow during calculation and targeted mesh refinement based on die geometry and mesh windows was used. This meant that the minimum element size was initially 0.14 mm and it decreased to 0.12 mm by the end of the simulation. The Siebel (or shear) friction model was applied to the contact with a factor of 0.12 based on previous, project results from internal studies with industrial partners, which is

also in agreement with default values for well lubricated cold forging. The punch was simplified to a restriction of vertical movement of the nodes in the top face of the billet and tool movement was simulated by moving the die upward at a speed of 10 mm/s. A stroke value of 13.2 mm of the die was set as the stopping condition. A die displacement-based step definition with 0.01 mm/step was defined in line with the recommendations of the DEFORM user's manual. Remeshing was activated and a relative interference depth of 0.7 times and a stretch limit of 1.3 times the element length were selected as remeshing triggers. The Spooles sparse solver in conjunction with the Newton-Raphson iteration method were employed. All other parameters were kept by default. In the second simulation step, the results are imported from the extrusion operation and a disc-shaped ejector object is added. A 10 mm/s ejection speed is applied and a 70 mm stroke stopping condition is used for full part ejection. During this step, the part is let to cool by conduction with the tool and convection with the environment using a default value for the convection coefficient of 0.02 N·mm/(s·ºC). After this, a new cooling operation is chained which inherits the results of the ejection, fixes three nodes and ends when all nodes cool below 30ºC.

3.2.2. DESCRIPTION OF THE SIMULATION OF MILLING USING BOOLEAN OPERATIONS

Due to the expected out-of-plane distortions, the 45º slice was transformed into the 360º complete specimen using a mirroring operation. The part was then remeshed to reduce element count and eliminate potential discontinuities. After this, a boolean step was added to the chain of the model and cutter geometries were introduced. These are idealized versions of the milled geometries with the same dimensions (see Fig. 3). The boolean operations at different depth were applied to the original geometry due to difficulties of remeshing in trials with chained boolean operations. The geometrical-based boolean method of DEFORM was used for remeshing the newly created surfaces after removing the material. Finally, a new relaxation step was created in which the parts distorted torsionally. For quantifying the FEM distortions Zeiss Inspect was once again used. In this case, no alignment was required as the meshes were already perfectly aligned at the alignment reference geometries and the distortions at the tip of the extruded zone could be clearly observed.

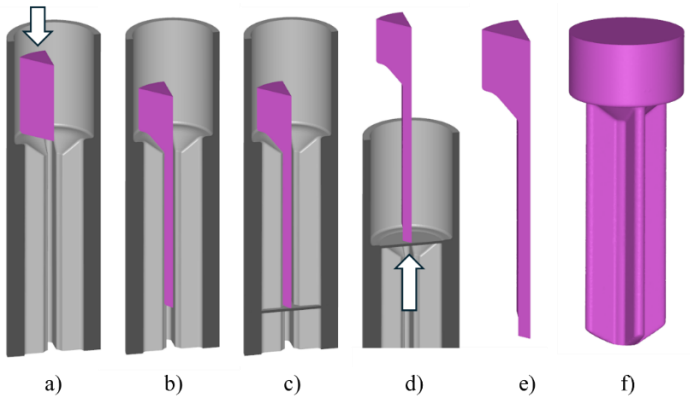

Fig. 6. Sequence of FEM simulation steps in DEFORM 3D. Start of extrusion (a), end of extrusion (b), start of ejection (c), end of ejection (d), relaxation and cooling (e), and mirroring and remeshing (f)

4. RESULTS AND DISCUSSION

In Fig. 7a, an example of a post-processed 3D scan ready for alignment is shown. In Fig. 7b an example of a deviation map between the milled specimens and the CAD model of the extruded part is presented. This map was created using the "surface comparison on actual" tool in Zeiss Inspect 2026. The positive deviations, shown in warm colours tending to red, are areas where the scanned specimen is over the surface of the CAD reference, while the colder, bluer zones, represent zones where the actual part is under the surface of the CAD. As it can be observed, the reference geometries show good alignment, with close-to-zero geometric deviation (represented by green colour). At the tip, on the side of the blades opposite to the milling operations, positive deviations can be seen while on the other side, either negative or almost zero deviation is observed. This means torsional distortions are present at the tip of the extrusion in the direction of milling depth. In Fig. 8 the magnitudes of the average blade tip deflections are plotted for the different tested specimens as a function of milling depth. Each point is the result of averaging the maximum positive blade tip deviations on all blades of the same specimen after milling at the established depths. The values were extracted by manual probing. Specimen 11 at 1.5 mm milling depth could not be properly aligned. Some of the specimens showed asymmetries in the values of positive deflection at the blade tips. These could be seen as relatively high deviations on a single blade and relatively small ones on the opposite one, which could be explained by misalignments of the scans to the CAD. However, all specimens, regardless of milling position, showed a general trend of torsional distortion with positive blade tip deviations from CAD ranging from 0.01 to 0.09 mm (with most being inside the range 0.01-0.04 mm) and small differences from blade to blade.

An unexpected observation is that blade tip deflections seem to "saturate" at higher milling depth, contrary to the initial hypothesis that higher milling depth would correlate with ever higher deflection. It is hypothesized that this is due to the higher surface strain hardening generally associated with extrusion processes due to friction and faster cooling at the contact surfaces with the die. The higher strain hardening could produce higher RS close to the surface, which when removed generate higher deflections. A detailed metallographic investigation of the variation in microhardness of the blades in both depth and longitudinal directions could be useful to validate this hypothesis. Another validation method would be the use of the layer removal method discussed in section 2 combined with XRD or other RS measurement techniques. Regarding the low value of the deviations and the asymmetries observed in some scans, a more robust and precise alignment strategy and a more precise and repeatable clamping or the specimens and CNC milling of the blades is required. In Fig. 9a-c, three simulation examples of milling operations using a depth of 1 mm for the boolean cuts are presented. Fig. 9d-f show the deviation maps created in Zeiss Inspect between the 360º extruded geometry from Fig. 6f and the relaxed boolean cuts of Fig. 9a-c. The torsional distortions can be clearly inferred from the positive deviations on the blade tip surfaces opposite the milled sides and the slight negative ones on the same faces where the parts were cut. In Fig. 8, the FEM maximum positive blade tip deviations are plotted in light orange as a function of milled depth and compared with the experiments. First of all, the same twisting direction of torsional deflection is predicted (in the direction of increasing milling depth). The "saturation" behaviour commented on before also seems to be captured by the simulations, as

higher boolean depths either present the same blade tip deflection or even slightly lower values (as in the bottom half case in Fig. 8). Additionally, the predicted blade tip deviations fall in the same range of the experimentally measured ones. In general, differences of approximately 22% (excluding a minority of cases that presented higher differences) in average blade tip deflection can be seen between FEM and experiments, which indicates good correlation.

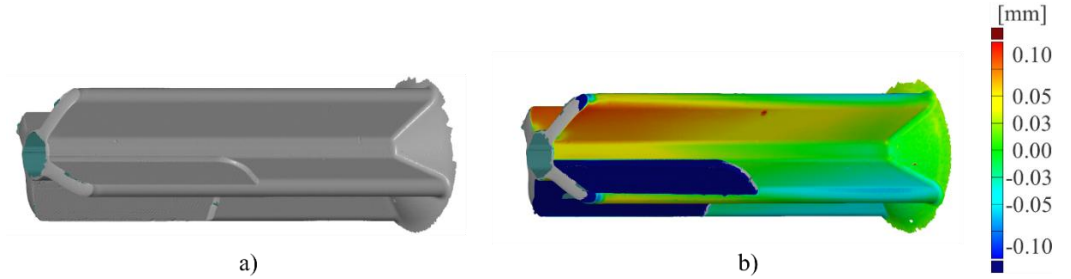

Fig. 7. Comparison of raw 3D scan (a) and example of surface comparison map in Zeiss Inspect (b)

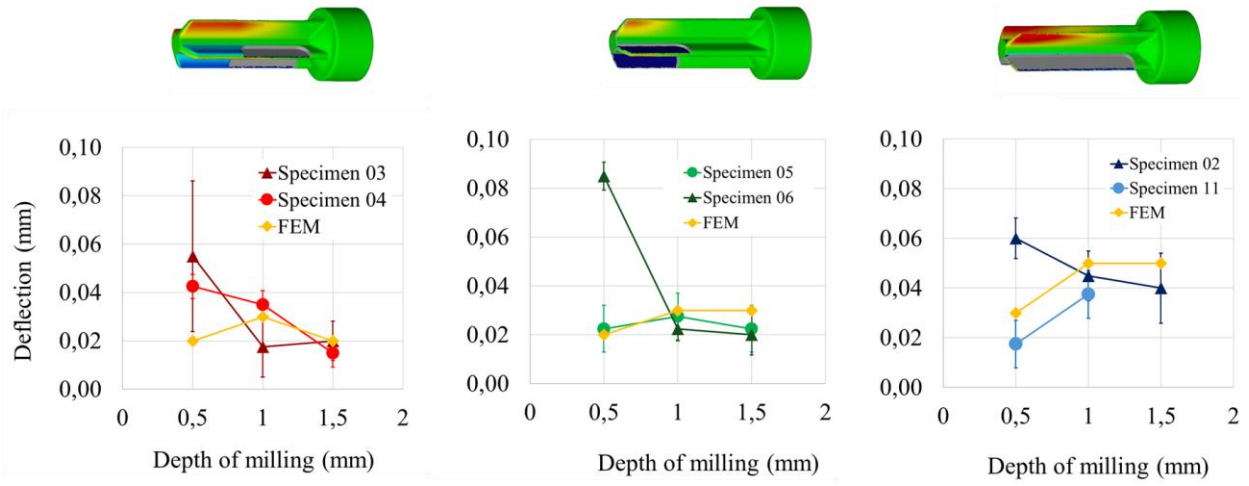

Fig. 8. Average blade tip deflection at different milling depths and milled geometries for experimental and FEM cuts

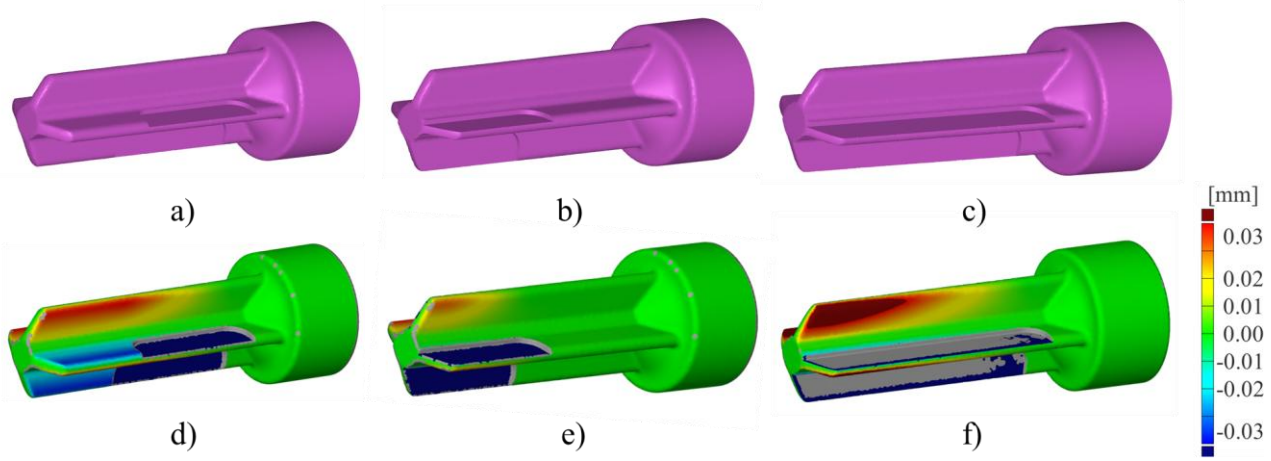

Fig. 9. Geometries of the components after boolean operations (a, b and c) and surface comparison with deflection plot compared to reference in Fig. 6f (d, e and f)

5. CONCLUSION AND OUTLOOK

In the present work, the capabilities of the commercial FEM software DEFORM for the prediction of the distortions generated by the liberation of BRS in EN AW-6082 aluminium specimens after targeted milling were assessed. The components were manufactured using cold forward extrusion. They were then systematically milled on the same faces of all blades at different areas and depths. All specimens were 3D scanned prior and after milling, and the 3D scans were aligned using the local best fit algorithm of Zeiss Inspect 2026 based on reference geometric features. Both the extrusion and milling processes were simulated in realistic and simplified ways respectively using the FEM program DEFORM 3D. The FEM-predicted milling-induced distortions were compared with experimentally measured distortions.

The following conclusions were extracted from the present investigation:

- RS fields are a complex property of formed components that have a significant influence on downstream processes such as milling. These are influenced by a wide variety of factors including friction with the forming die, determined by die geometry and billet lubrication, thermal considerations such as heat generation from friction and plastic deformation, cooling rates due to conduction with the forming tools and convection with the environment, etc. In order to accurately predict RS fields, and their effects, all such factors and their complex interactions must be taken into account using empirically-calibrated parameter values.
- The targeted milling of extruded and bladed geometries in a cyclically symmetric pattern produces torsional distortions of the component in the milling depth direction measured by blade tip deflections in the overall range of 0.01 to 0.09 mm with most measurements falling in the range of 0.01 and 0.04 mm. These distortions have been both qualitatively predicted in terms of the direction of blade tip deflection and in quantitative terms, as the FEM-predicted blade tip deflections differ from experimental comparisons between 3D scans of milled parts and a CAD reference by 22% on average (with a small minority of discarded outliers varying up to 325%, which are not considered to invalidate the results). The average difference between simulation and experiments of 22% is considered low enough so that the simulations adequately capture the behaviour of the empirical data. This agreement between the simulations and experiments means that based on the employed methodology, DEFORM 3D can adequately predict milling-induced distortions caused by the liberation of BRS in cold forged specimens.
- The low values of distortion measured require a very precise clamping and alignment of the 3D scans of the parts before and after milling. The strategy used in the present investigation present some important limitations such as digitalization defects, incomplete part scanning, lack of proper alignment between reference and milled scans, which required the use of a CAD model as a reference to align to. In order to confidently determine the distortion patterns and magnitudes in the specimens after milling, the alignment accuracy and precision must be improved.

5.1. OUTLOOK AND FUTURE STUDIES

Some improvements to the present methodology are here proposed, as well as lines of future investigation based on the results and conclusions. The predictive capabilities of the RS fields themselves (not only their effects) and comparison with experimental measurement of those fields is an obvious path forward from the present investigation. A more robust clamping and alignment strategy can be used to improve confidence in the measured distortions. A clamping solution valid for both milling and digitalization of the geometry, so that the component stays clamped and aligned during all phases of processing, would be a more robust strategy. The use of more precise CNC machining centres would increase the repeatability of cuts between blades and specimens. In terms of FEM simulations, more accurate, even experimentally calibrated, values for the coefficient of friction (both in extrusion and ejection), interface heat transfer coefficient, part dwell times in the die, etc. could improve the accuracy of prediction of the distortions. A sensitivity analysis for the determination of the most influential factors is essential to this end.

Also, the application of a MIRS field as a nodal BC to the new surfaces created by the boolean operation could allow for more accurate prediction of machining-induced deflections. This could be done using simplified tools like DEFORM's machining distortion module or by applying realistic chip formation simulations to only certain 2D slices of the formed part and then interpolating between them to generate a continuous approximation of the MIRS field. Further future investigations could involve the determination of actual depth maps of RS by using techniques such as the layer removal method combined with XRD measurement for a 3D mapping of BRS, the use of more accurate RS-measuring methods like neutron diffraction, the application of strain gauges for in-situ, real-time measurement of part deflection during milling or the application of the study to a more complex geometry generated by twisting the blades and machining a simplified, four-blade impeller-like geometry.

REFERENCES

[1] KRETZ T., HERRMANN T., GRÖTZINGER K.C., MATEI R.A., LIEWALD M., 2025, *Heliform – Einstufiges Fließpressen Helixförmiger Near-Net-Shape-Verdichterräder*, EN AW-6082, massivUMFORMUNG, 09/2025, 44–49.

[2] AKHTAR W., LAZOGLU I., LIANG S.Y., 2022, *Prediction and Control of Residual Stress-Based Distortions in the Machining of Aerospace Parts: A Review*, Journal of Manufacturing Processes, 76, 106–122.

[3] LI J., WANG S., 2017, *Distortion Caused by Residual Stresses in Machining Aeronautical Aluminium Alloy Parts: Recent Advances*, The International Journal of Advanced Manufacturing Technology, 89, 997–1012.

[4] TEKKAYA A.E., ALLWOOD J.M., BARIANI P.F., BRUSCHI S., CAO J., GRAMLICH S., GROCHE P., HIRT G., ISHIKAWA T., LÖBBE C., LUEG-ALTHOFF J., MERKLEIN M., MISIOLEK W.Z., PIETRZYK M., SHIVPURI R., YANAGIMOTO J., 2015, *Metal Forming Beyond Shaping: Predicting and Setting Product Properties*, CIRP Annals, 64/2, 629–653.

[5] TEKKAYA A.E., GERHARDT J., 1985, *Residual Stresses in Cold-Formed Workpieces*, CIRP Annals, 34/1, 225–230.

[6] ARRAZOLA P.J., ÖZEL T., UMBRELLO D., DAVIES M., JAWAHIR I.S., 2013, *Recent Advances in Modelling of Metal Machining Processes*, CIRP Annals, 62/2, 695–718.

[7] WÖSTE F., KIMM J., BERGMANN J.A., THEISEN W., WIEDERKEHR P., 2021, *Investigation of the Effect of Residual Stresses in the Subsurface on Process Forces for Consecutive Orthogonal Cuts*, Production Engineering, 15/6, 873–883.
[8] SHI D.-M., HUANG T., ZHANG X.-M., DING H., 2022, *An Explicit Coupling Model for Accurate Prediction of Force-Induced Deflection in Thin-Walled Workpiece Milling*, Journal of Manufacturing Science and Engineering, 144/8, 081005.
[9] BRINKSMEIER E., SÖLTER J., 2009, *Prediction of Shape Deviations in Machining*, CIRP Annals, 58/1, 507– 510.
[10] LIU L., SUN J., CHEN W., SUN P., 2017, *Study on the Machining Distortion of Aluminium Alloy Parts Induced by Forging Residual Stresses*, Proceedings of the Institution of Mechanical Engineers, Part B: Journal of Engineering Manufacture, 231/4, 618–627.
[11] HASAN M.M., SCHOOP J., 2023, *Physics-Informed Uncertainty Quantification in Modelling of Machining Induced Residual Stress*, Procedia CIRP, 117, 139–144.
[12] ALLWOOD J.M., DUNCAN S.R., CAO J., GROCHE P., HIRT G., KINSEY B., KUBOKI T., LIEWALD M., STERZING A., TEKKAYA A.E., 2016, *Closed-Loop Control of Product Properties in Metal Forming*, CIRP Annals, 65/2, 573–596.
[13] RAMME J., WEGERT R., GUSKI V., SCHMAUDER S., MOEHRING H.-C., 2022, *Development of a Multi-Sensor Concept for Real-Time Temperature Measurement at the Cutting Insert of a Single-Lip Deep Hole Drilling Tool*, Applied Sciences, 12/14, 7095.
[14] WEGERT R., GUSKI V., SCHMAUDER S., MOEHRING H.-C., 2024, *In-Process Approach for Editing the Subsurface Properties During Single-Lip Deep Hole Drilling Using a Sensor-Integrated Tool*, Production Engineering, 18/2, 319–337.
[15] GEORGI P., ESCHELBACHER S., MOEHRING H.-C., 2021, *Utilization of Machine Learning Approaches for Tool Wear Detection and Prediction in the Circular Sawing Process of Metallic Materials*, MM Science Journal, 2021/5, 5120–5125.
[16] REEBER T., WOLF J., MOEHRING H.-C., 2024, *A Data-Driven Approach for Cutting Force Prediction in FEM Machining Simulations Using Gradient Boosted Machines*, Journal of Manufacturing and Materials Processing, 8/3, 107.
[17] DENKENA B., DE LEON L., 2008, *Milling-Induced Residual Stresses in Structural Parts Out of Forged Aluminium Alloys*, Int. J. Machining and Machinability of Materials, 4/4, 335–344.
[18] WEBER D., KIRSCH B., CHIGHIZOLA C. R., D'ELIA C. R., LINKE B. S., HILL M. R., AURICH J. C., 2021, *Analysis of Machining-Induced Residual Stresses of Milled Aluminium Workpieces, Their Repeatability, and Their Resulting Distortion*, Int. J. Adv. Manuf. Technol., 115, 1089–1110.
[19] CHIGHIZOLA C. R., D'ELIA C. R., WEBER D., KIRSCH B., AURICH J. C., LINKE B. S., HILL M. R., 2021, *Intermethod Comparison and Evaluation of Measured Near Surface Residual Stress in Milled Aluminium*, Exp. Mech., 61/8, 1309–1322.
[20] JI C., SUN S., LIN B., FEI J., 2018, *Effect of Cutting Parameters on the Residual Stress Distribution Generated by Pocket Milling of 2219 Aluminium Alloy*, Advances in Mechanical Engineering, 10/12, 1–15.
[21] ZAWADA-MICHALOWSKA M., PIESKO P., MROWKA-NOWOTNIK G., NOWOTNIK A., LEGUTKO S., 2024, *Effect of the Technological Parameters of Milling on Residual Stress in the Surface Layer of Thin-Walled Plates*, Materials, 17/5, 1193.
[22] ZAWADA-MICHALOWSKA M., ANASIEWICZ K., KORPYSA J., PIESKO P., 2025, *Experimental Investigation of the Influence of Milling Conditions on Residual Stress in the Surface Layer of an Aerospace Aluminium Alloy*, Materials, 18/4, 811.
[23] WAN M., YE X.-Y., YANG Y., ZHANG W.-H., 2017, *Theoretical Prediction of Machining-Induced Residual Stresses in Three-Dimensional Oblique Milling Processes*, Int. J. Mech. Sci., 133, 426–437.
[24] DEL PRETE A., FRANCHI R., ANTERMITE F., DONATIELLO I., 2018, *Numerical Simulation of Machining Distortions on a Forged Aerospace Component Following a One and a Multi-Step Approaches*, AIP Conference Proceedings, 1960/1, 070009.
[25] CERUTTI X., MOCELLIN K., 2015, *Parallel Finite Element Tool to Predict Distortion Induced by Initial Residual Stresses During Machining of Aeronautical Parts*, International Journal of Material Forming, 8/3, 255–268.
[26] MA K., GOETZ R., SRIVATSA S.K., 2010, *Modelling of Residual Stress and Machining Distortion in Aerospace Components*, FURRER D.U., SEMIATIN S.L. (Eds.), ASM Handbook, 22B, Metals Process Simulation, ASM International, 386–407.